Dehydration of Xylose to Furfural and Its Valorization via Different Multicomponent Reactions Using Sulfonated Silica with Magnetic Properties as Recyclable Catalyst

José J. Martínez, Eliana Nope, Hugo Rojas, Jairo Cubillos, Ángel G. Sathicq & Gustavo P. Romanelli

VOLUME 144 (2014)
No. 6

ISSN 1011-372X
Published June 2014

CATALYSIS LETTERS

Springer

Springer

Springer

Dehydration of Xylose to Furfural and Its Valorization via Different Multicomponent Reactions Using Sulfonated Silica with Magnetic Properties as Recyclable Catalyst

José J. Martínez · Eliana Nope · Hugo Rojas ·
Jairo Cubillos · Ángel G. Sathicq · Gustavo P. Romanelli

Abstract Sulfonated silica with magnetic properties was studied for dehydration of xylose to furfural and posteriorly for furfural valorization through the Biginelli and Hantzsch multicomponent reactions. Eleven polysubstituted heterocycles were obtained in excellent yields and without any side-product (81–91 %), using a multicomponent green methodology. The presence of Fe_3O_4 particles allows an easy separation from the reaction medium giving a high yield in the reusability studies.

J. J. Martínez (✉) · E. Nope · H. Rojas · J. Cubillos
Escuela de Ciencias Químicas, Facultad de Ciencias,
Universidad Pedagógica y Tecnológica de Colombia UPTC,
Avenida Central del Norte, Vía Paipa, Tunja, Boyacá, Colombia
e-mail: jose.martinez@uptc.edu.co

E. Nope
e-mail: eliana.nope@uptc.edu.co

H. Rojas
e-mail: hugo.rojas@uptc.edu.co

J. Cubillos
e-mail: jairo.cubillos@uptc.edu.co

Á. G. Sathicq · G. P. Romanelli
Departamento de Química, Facultad de Ciencias Exactas, Centro
de Investigación y Desarrollo en Ciencias Aplicadas "Dr. J.J.
Ronco" (CINDECA), UNLP-CCT-CONICET. Calle 47 N° 257,
B1900AJK La Plata, Argentina
e-mail: agsathicq@quimica.unlp.edu.ar

G. P. Romanelli
e-mail: gpr@quimica.unlp.edu.ar

1 Introduction

Hydrolysis of lignocellulosic biomass can lead to hexoses (glucose and fructose) and pentoses (xylose), and the dehydration of these sugars to 5-hydroxymethylfurfural (HMF) and 2-furfural (FAL). Both HMF and FAL are building blocks widely applicable for the next generation of biofuels, bio-based plastics, adhesive monomers, ecological adhesives, coating agents and fine chemical products [1]. The dehydration of xylose to furfural requires a high temperature and the presence of a strong acid as catalyst (Fig. 1). Conventional acid liquid catalysts (H_2SO_4, HCl, and H_3PO_4) have been proven as efficient catalysts for various industrial processes by virtue of their higher Ka values and their efficient interaction with the reactant molecules [2]. However, they generate corrosion problems in the reactor and require special processing in the form of neutralization [3], which involves costly and inefficient catalyst separation from homogeneous reaction mixtures imposing environmental and economic barriers at industrial scale [4].

The need for a "green" approach to chemical processing has stimulated the use of recyclable strong acid solids as replacements for unrecyclable liquid acid catalysts such as H_2SO_4 [5]. The acid solid particles can be readily separated from liquid products by decantation or filtration, and the catalyst can be used repeatedly for the reaction without neutralization, minimizing energy consumption and waste generation. Heterogeneous catalysis may potentially provide simpler and more environmentally friendly processes due to the easy separation and recyclability of the catalyst. Thus, acid solids such as zeolites, mesoporous [6] and ion-exchange polymers [7] could replace homogeneous acids. In these solids, the Brönsted-type acidity should be a requirement. Acid solid catalysts with sulfonic groups
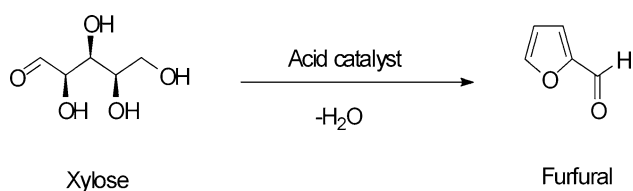
Fig. 1 Xylose dehydration to furfural

allow glycosidic bonds to efficiently hydrolyze β-1,4, [4], [8], being an useful tool in the chemical transformation of compounds of lignocellulosic biomass to high value-added products [9]. Both SiO_2 and Al_2O_3 have been used as supports for functionalization with sulfonic groups, and have been studied in distinct organic reactions [7, 10–12].

To address the issue of reuse, sulfonated solid catalysts with magnetic properties have been used [13, 14]. The paramagnetic properties of the solids allow easy separation of the catalyst in the reaction mixture using an external magnetic field [15–17]. Aggregation of the particles can be avoided by the use of stabilizers or by the formation of a passive layer of silica or other oxide on the surfaces of nanoparticles (NPs) of iron oxide [18].

On the other hand, the generation of molecular complexity and diversity from very simple substrates, while combining environmental aspects with economic ones, represents a great challenge in modern organic chemistry, both from academic and industrial points of view. Multicomponent reactions involving domino processes have emerged as powerful tools to reach this near ideal goal [19, 20]. Two interesting multicomponent reactions due to their versatility are the Hantzsch and Biginelli reactions and they are key to obtain nitrogenated polysubstituted heterocycles such as 3,4-dihydropyrimidin-2(1H)-ones (thiones), trifluoromethylated-hexafluoropyridin-2(1H)-ones (thiones), and 1,4-dihydropyridines. 3,4-dihydropyrimidin-2(1H)-ones (thiones) are interesting compounds in the fields of therapeutics and bioorganic chemistry. Their compounds exhibit a wide spectrum of biological activity as well as antibacterial, anti-inflammatory, antifungal, antiviral, anticancer, and antihypertensive properties [21]. The Biginelli reaction is a multicomponent reaction that involves an acid-catalyzed cyclocondensation of β-dicarbonyl compounds, aldehydes, and urea or thiourea [22]. A number of synthetic procedures for preparing 3,4-dihydropyrimidin-2-(1H)-ones (thiones) involve catalysis by protic acids such as concentrated H_2SO_4 and HCl, a variety of Lewis acids such as $CeCl_3.7H_2O$ and $LiClO_4$, and recoverable catalysts, ion-exchange resins, and heteropolyacids [23].

In 1999, Oliver Kappe and coworkers discovered that by the use of a fluorinated acetoacetic ester derivative (ethyl

trifluoromethylacetoacetate), the Biginelli reaction takes a different course and trifluoromethylated hexahydropyridimidinones are obtained [23]. The hexahydropyrimidine nucleus is present in a number of alkaloids, such as tetraponerines and verbametrine. The preparation method of hexahydropyrimidinones involves the use of the same catalyst as the one used for the synthesis of 3,4-dihydropyrimidin-2(1H)-ones, for example, HCl, p-toluenesulfonic acid, or sulfamic acid [24].

1,4-Dihydropyrimidines are six-member heterocycles that exhibit various activities, for example, calcium channel antagonist, antitumor, anti-inflammatory, analgesic, antihypertensive, and antianginal activity [25]. The classical methods involve the three-component condensation of aldehydes with β-dicarbonyl compounds and ammonia. Several catalysts have been reported for this synthesis, such as molecular iodine, ionic liquids, silica gel/$NaHSO_4$, TMSCl–NaI, and heteropolyacids [23].

In this study, solid acid catalysts with sulfonic groups were studied in the conversion of xylose to furfural. Besides, to show the versatility of the furfural molecule as building block we used it as substrate in the Biginelli and Hantzsch-type multicomponent reactions to obtain different polyfunctional nitrogenated heterocycles using green protocols (Fig. 2), including a solvent-free reaction and a recyclable solid acid with magnetic properties (Fe_3O_4/SiO_2–SO_3H) that is easily separable from the reaction medium [14]. Although Biginelli and Hantzsch-type multicomponent reactions has been studied with acid solids with magnetic properties (Fe_3O_4–SO_3H) [26–28], the valorization of the furfural obtained from xylose dehydration using magnetic sulfonated silica (Fe_3O_4/SiO_2–SO_3H) has scarcely been reported. In this sense, the present study points to accumulate data on the catalytic behavior of this material in the furfural production chain.

2 Experimental

2.1 Catalyst Preparation

2.1.1 Synthesis of SiO_2–SO_3H

A mixture of 5 g of SiO_2 (Syloid S_{BET} = 283 m^2/g) in 100 mL of dry toluene, and 3-mercaptopropyltrimethoxysilane (MPTMS) (1.15 mL, 6.1 mmol) was refluxed for 24 h. The solid obtained was washed with toluene and dried at 363 K. Subsequently, mercaptopropyl groups were oxidized to sulfonic acid groups with excess hydrogen peroxide at room temperature for 24 h, a few drops of H_2SO_4 were added within 12 h, and the solid was washed with acetone and dried at 393 K.

Fig. 2 Furfural valorization in multicomponent reactions
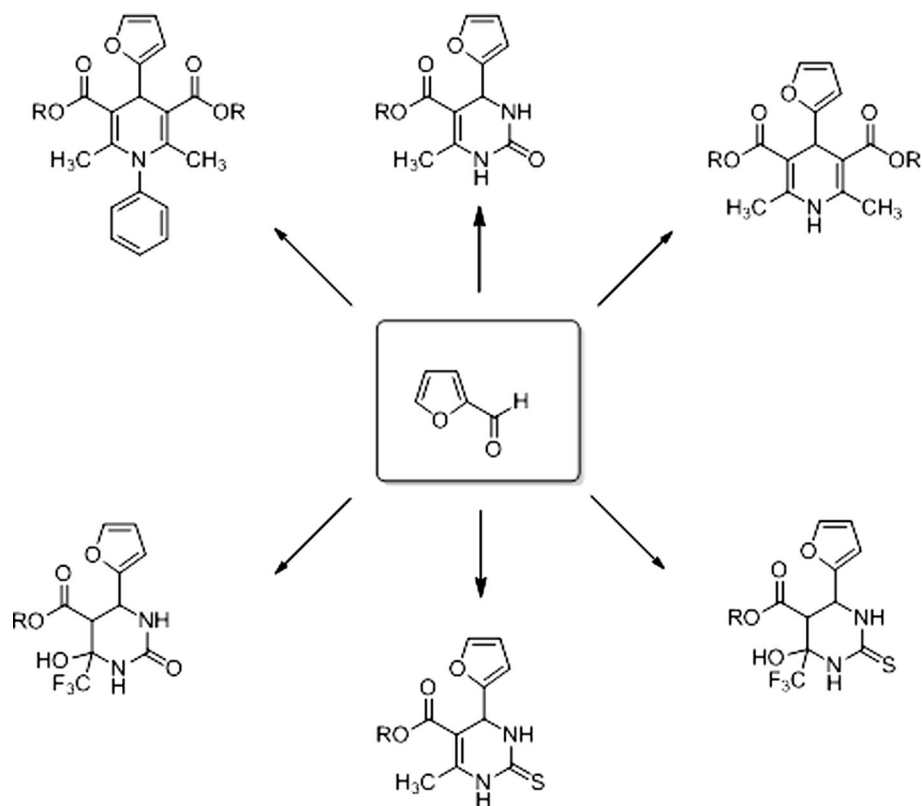
2.1.2 Synthesis of Fe₃O₄ Particles

The magnetic NPs were synthesized by the co-precipitation method using the methodology proposed by Kang et al. [29] A molar ratio of Fe(II)/Fe(III) = 0.5 and a pH 11–12 were used. Briefly, 0.85 mL of 12.1 N HCl and 25 mL of purified, deoxygenated water (by nitrogen gas bubbling for 30 min) were combined, and 5.2 g of FeCl₃ and 2.0 g of FeCl₂ were successively dissolved in the solution with stirring. The resulting solution was added dropwise to 250 mL of 1.5 M NaOH solution under vigorous stirring, generating a black precipitate, which was then centrifuged at 4,000 rpm and washed with deoxygenated water. Subsequently, 500 mL of 0.01 M HCl was added to neutralize the anionic charges on the NPs. The solid was obtained by centrifugation, washed again with distilled water and then dried at 353 K.

2.1.3 Encapsulation of Fe₃O₄ on SiO₂

The encapsulation process of the magnetic microspheres with SiO₂ was performed by the Stöber method [30]; in a typical process, 0.5 g Fe₃O₄ particles were dispersed in a mixture of ethanol (200 mL), deionized water (100 mL), and concentrated ammonia aqueous solution (6 mL) by ultrasonication for 1 h. Subsequently, 1.75 mL of tetraethyl orthosilicate was added dropwise and stirred for 3 h.

The product was filtered, washed with deionized water and then dried under vacuum at 343 K for further use. The relationship between the magnetic particles and the source of silica was 1:1.

2.1.4 Synthesis of Fe₃O₄–SiO₂–SO₃H

The functionalization of Fe₃O₄–SiO₂ with MPTMS and its subsequent oxidation with H₂O₂ were followed using the methodology described in Sect. 2.1.1. The solids obtained were called Fe₃O₄–SiO₂–SO₃H.

2.2 Catalyst Characterization

X-ray diffraction patterns were collected on a PANalytical X-Pert-Pro diffractometer using Ni filter and Cu kα radiation ($\lambda = 1.54056$ Å). The spectra were obtained in the range 20–85° using a scan rate of 0.01° and 0.04° s⁻¹, respectively.

The textural properties, which were determined from nitrogen adsorption at 77 K, were measured on Micromeritics ASAP 2020 equipment. Samples were previously evacuated at 623 K for 16 h. The surface area was calculated using a multipoint Brunauer-Emmett-Teller model. The pore size distribution was obtained by the BJH model, and the total pore volume was estimated at a relative pressure of 0.99.

Magnetization measurements were performed on a vibrating sample magnetometer—VersaLab at 300 K. FTIR in ATR mode was used to determine the presence of –SO₃H groups using a Nicolet iS50 Analytical FTIR Spectrometer.

The acid capacity was determined by titration with 0.01 M NaOH (*aq*) [31]. In a typical experiment, 0.1 g of solid was added to 10 mL of deionized water. The resulting suspension was allowed to equilibrate and thereafter was titrated by dropwise addition of 0.01 M NaOH solution using phenolphthalein as pH indicator.

2.3 Catalytic Studies of Xylose Dehydration

Sulfonated solids were evaluated in the dehydration reaction of xylose. In a typical experiment, 0.9 g xylose, 0.1 g catalyst and 30 mL deionized water were placed in a batch reactor at 400 rpm and 343 K. After 3 h, the catalyst was separated by filtration. The catalyst-free liquid mixture was analyzed by high resolution liquid chromatography with refractive index detector using a C4-propyl column. The magnetic solids were reused in the three cycles of reaction.

2.4 Furfural Valorization in the Multicomponent Synthesis

All chemicals were purchased commercially and used without further purification. Melting points were measured in an open capillary using Buchi melting point apparatus and were uncorrected. ¹H NMR and ¹³C NMR spectra were recorded on a Bruker AM-400 spectrometer (400 and 100 MHz, respectively) using TMS as internal standard. Gas chromatography was recorded on a Shimadzu CG 2010 instrument.

2.4.1 General Procedure for the Synthesis of 3,4-Dihydropyrimidin-2(1H)-ones (thiones)

2.4.1.1 Representative Procedure for the Synthesis of 5-Ethoxycarbonyl-4-(2-furfuryl)-6-methyl-3,4-dihydropyrimidin-2(1H)-one A mixture of ethyl acetoacetate (130 mg, 1 mmol), furfural (96 mg, 1 mmol), urea (90 mg, 1.5 mmol), and Fe₃O₄/SiO₂–SO₃H (25 mg) was thoroughly mixed and then heated at 80 °C for 1.5 h. The progress of the reaction was monitored by TLC. After completion of the reaction, acetone was added (2 × 1 mL) and the catalyst was filtered. The extracts were combined and dried with anhydrous sodium sulfate and concentrated in vacuum (50 °C). The crude product was recrystallized from methanol or isopropanol to give pure 5-ethoxycarbonyl-4-(2-furfuryl)-6-methyl-3,4-dihydropyrimidin-2(1H)-one (compound 1).

2.4.1.2 Recycling of the Catalyst The reaction was carried out as stated previously; the reaction mixture was stirred with acetone and then the acetone solution was filtered from the insoluble catalyst (three times, 1 mL each). The catalyst was dried under vacuum (50 °C) and reused, repeating this procedure.

2.4.2 General Procedure for the Synthesis of Trifluoromethylated hexahydropyrimidin-2(1H)-ones (thiones)

2.4.2.1 Representative Procedure for the Synthesis of 5-Ethoxycarbonyl-4-(2-Furfuryl)-6-hydroxy-6-trifluoromethyl-hexahydropyrimidin-2(1H)-one A mixture of ethyl-trifluoroacetoacetate (184 mg, 1 mmol), furfural (96 mg, 1 mmol), urea (90 mg, 1.5 mmol), and Fe₃O₄/SiO₂–SO₃H (25 mg) was thoroughly mixed and then heated at 80 °C for 1.5 h. The progress of the reaction was monitored by TLC. After completion of the reaction, acetone was added (2 × 1 mL) and the catalyst was filtered. The extracts were combined and dried with anhydrous sodium sulfate and concentrated in vacuum (50 °C). The crude product was recrystallized from methanol or isopropanol to give pure 5-ethoxycarbonyl-4-(2-Furfuryl)-6-hydroxy-6-trifluoromethyl-hexahydropyrimidin-2(1H) one (compound 5).

2.4.3 General Procedure for the Synthesis of 1,4-Dihydropyrimidines

2.4.3.1 Representative Procedure for the Synthesis of 2,6-Dimethyl-4-(2-furfuryl)-1,4-dihydro-pyridine-3,5-dicarboxylic acid diethyl ester A mixture of ethyl acetoacetate (260 mg, 2 mmol), furfural (96 mg, 1 mmol), ammonium acetate (103 mg, 1.2 mmol), and Fe₃O₄/SiO₂–SO₃H (25 mg) was thoroughly mixed and then heated at 80 °C for 1 h. The progress of the reaction was monitored by TLC. After completion of the reaction, acetone was added (2 × 1 mL) and the catalyst was filtered. The extracts were combined and dried with anhydrous sodium sulfate and concentrated in vacuum (50 °C). The crude product was recrystallized from methanol or isopropanol to give pure 1,4-dihydropyridine.

2.4.4 Melting Points and Spectral Data for Representative Products

2.4.4.1 5-Ethoxycarbonyl-4-(2-furfuryl)-6-methyl-3,4-dihydropyrimidin-2(1H)-one, (*2*) Yield: 90 %; mp 209–211 °C (lit. [32] 209–211 °C); ¹H NMR: δ = 9.27 (s, 1H), 7.74 (s, 1H), 7.54 (s, 1H), 6.34 (s, 1H), 6.08 (s, 1H), 5.20 (s, 1H), 4.02 (q, J = 7 Hz, 2H), 2.20 (s, 3H), 1.11 (t, J = 7 Hz, 3H); ¹³C NMR: δ = 165.1, 155.8, 152.4, 149.1, 142.0, 110.3, 105.1, 96.8, 59.2, 47.8, 17.7, 14.2.

2.4.4.2 5-Ethoxycarbonyl-4-(2-furfuryl)-6-methyl-3,4-di-hydropyrimidin-2(1H)-thione,(4) Yield: 82 %; mp 209–210 °C (lit. [33] 208–210 °C); ^{1}H NMR: δ = 1.20 (t, J = 7.2 Hz, 3H), 2.38 (s, 3H), 4.16 (m, 2H), 5.51 (s, 1H), 6.18 (d, J = 2.4 Hz, 1H), 6.32 (s, 1H), 6.96 S, 1H), 7.34 (s, 1H), 7.52 (s, 1H).

2.4.4.3 5-Ethoxycarbonyl-4-(2-furfuryl)-6-hydroxy-6-tri-fluoromethyl-hexahydropyrimidin-2(1H)-one, (5) Yields: 90 %; mp 98–100 °C (lit. [34] 96–100 °C); ^{1}H NMR: δ = 10.1 (s, 1H), 9.77 (s, 1H), 7,4 (s, 1H), 6.7–7.2 (m, 4H), 4.71 (d, J = 11 Hz, 2H), 3.82 (q, J = 7 Hz, 2H), 3.5 (d, J = 11 Hz, 1H), 1.25 (t, J = 7 Hz, 3 H).

2.4.4.4 5-Ethoxycarbonyl-4-(2-furfuryl)-6-hydroxy-6-tri-fluoromethyl-hexahydropyrimidin-2(1H)-thione, (6) Yields: (81 %); mp 80–82 °C (lit. [35] 80–83 °C); ^{1}H NMR: δ = 9.8 (s, 1H), 9.5 (s, 1H), 7.77 (s, 1H), 6.74–6.49 (m, 4H), 4.82 (d, J = 11 Hz, 1H), 3.75 (q, J = 7 Hz, 2H), 3.5 (d, J = 11 Hz, 1H), 0.97 (t, J = 7 Hz, 3H).

2.4.4.5 2,6-Dimethyl-4-(2-furfuryl)-1,4-dihydro-pyridine-3,5-dicarboxylic acid dimethyl ester, (7) Yields: 91 %; mp 187–190 °C (lit. [35] 188–190 °C); ^{1}H NMR: δ = 2.32 (s, 6H), 3.71 (s, 6H), 5.19 (s, 1H), 5.77 (s, 1H), 5.78 (m, 3H), 6.0 (s, 1H), 7.21 (s, 1H); ^{13}C NMR δ = 167.9, 158.4, 145.2, 141.1, 110.0, 104.2, 100.6, 51.1, 33.2, 19.5.

2.4.4.6 2,6-Dimethyl-4-(2-furfuryl)-1,4-dihydro-pyridine-3,5-dicarboxylic acid diethyl ester, (8) Yields: 90 %; mp 165–168 °C (lit. [35] 165–168 °C); ^{1}H NMR: δ = 1.16–1.40 (m, 6H), 2.24–2.32 (m, 6H), 4.05 (q, J = 9 Hz, 2H), 4.14 (q, J = 8.4 Hz, 2H), 5.11 (s, 1H), 5.86-6.16 (m, 3H), 7.13-7.18 (m, 2H); ^{13}C NMR δ = 14.2, 19.5, 33.4, 59.8, 100.3, 104.4, 110.3, 140.6, 143.7, 158.8, 167.5.

2.4.4.7 2,6-Dimethyl-4-(2-furfuryl)-1-phenyl-1,4-dihydro-pyridine-3,5-dicarboxylic acid diethyl ester (9) Yields: 85 %; mp 150–151 °C (lit. [36] 150–152 °C), ^{1}H NMR: δ = 1.21 (t, J = 7 Hz, 6H), 2.11 (s, 6H), 4.1 (q, J = 7 Hz, 4H), 5.2 (s, 4H), 6.2–6, (m, 3H), 7.3-7.7 (m, 5H).

3 Results and Discussion

3.1 Catalyst Synthesis and Characterization

The magnetic properties of the encapsulated and functionalized Fe_3O_4 NPs are shown in Fig. 3. It can be seen that all the curves pass through the origin, resulting in solids that do not present coactivity or remanence, which indicates their superparamagnetic behavior and therefore they can be easily dispersed when the applied magnetic
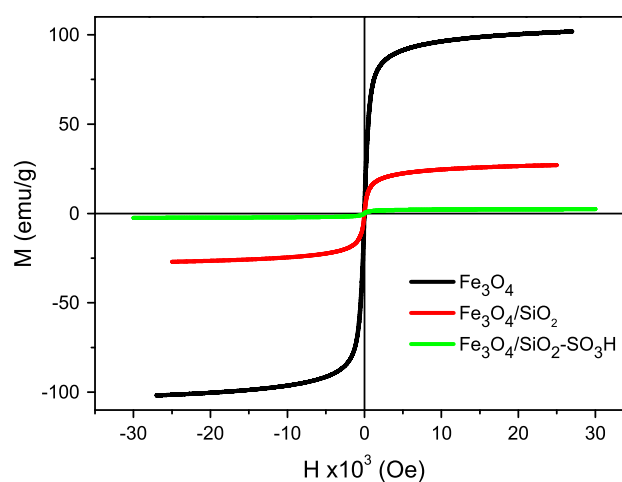

Fig. 3 Room temperature magnetic hysteresis loops of magnetic solids/Magnetic hysteresis loops of magnetic solids at room temperature
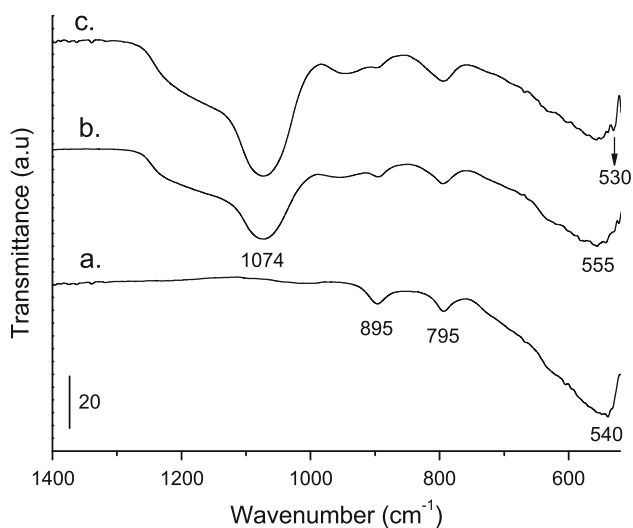
field is removed [37]. The magnetization saturation (Ms) values of Fe_3O_4 and Fe_3O_4/SiO_2 are 99 and 26 emu/g, respectively, which indicates that the SiO_2 coating affects this magnetic behavior. The magnetic response of Fe_3O_4/SiO_2 drops drastically when the solids are functionalized with MPTMS and further oxidized with H_2O_2; however, these solids can be easily separated from the reaction medium applying a strong magnetic field.

Figure 4 displays the diffraction patterns of Fe_3O_4, Fe_3O_4/SiO_2 and $Fe_3O_4/SiO_2–SO_3H$. Figure 4a shows the reflections characteristic of cubic inverse spinel Fe_3O_4 NPs (JCPDS 89-0950): however, $γ-Fe_2O_3$ (JCPDS 33-0664) has a crystal structure and 32 lattice spacing similar to that of Fe_3O_4. The difference between the experimental *d* value and the intensity of lines is because the XRD patterns correspond to Fe_3O_4 NPs. Several small peaks centered at 2θ angles of 33.2°, 41.2°, 59.0° and 61.4° indicate the occurrence of $α-FeOOH$, in addition to the predominant Fe_3O_4 phase. The reflection lines of Fe_3O_4 and $α-FeOOH$ are observed in all the other solids. Figure 4b exhibits a signal near 2θ = 22°, assigned to the amorphous silica, due to the silica coating in Fe_3O_4 NPs. This same signal is observed in Fe_3O_4/SiO_2-SO_3H (Fig. 4c). The crystal size of Fe_3O_4 using the (3 1 1) reflection peak at 2θ = 35.5° indicates that the crystallinity of Fe_3O_4 is retained during the functionalization of SiO_2 with –SO_3H groups.

Figure 5 shows the FTIR spectra of magnetic solids and the zone magnified from 1,400 to 400 cm^{-1}. The Fe_3O_4 sample (Fig. 5a) shows two IR bands at 895 and 795 cm^{-1} that can be assigned to Fe–O–H bending vibrations in $α-FeOOH$ [38]. These bands are usually used for the identification of $α-FeOOH$ in a qualitative phase analysis of iron oxide mixtures [39, 40]. The absorption band at 534 cm^{-1} is
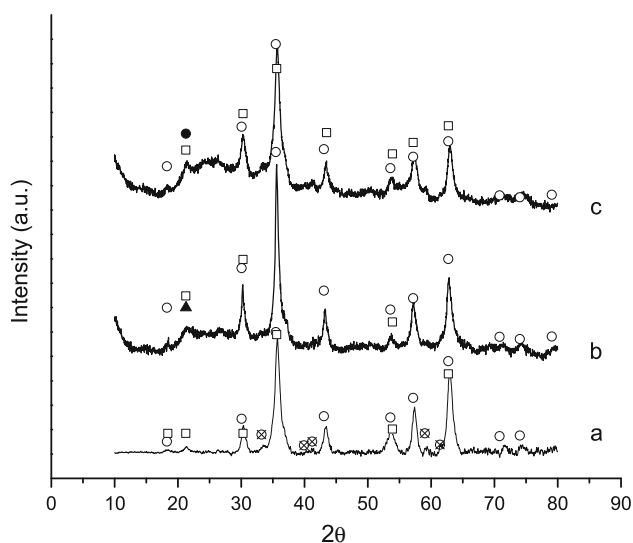
Fig. 4 X-ray patterns of the supported acid catalysts: *a* Fe$_3$O$_4$, *b* Fe$_3$O$_4$/SiO$_2$, *c* Fe$_3$O$_4$/SiO$_2$-SO$_3$H. Note: peak assignments: (*unfilled circle*) Fe$_3$O$_4$, (*unfilled square*) γ-Fe$_2$O$_3$, (*filled triangle*) SiO$_2$, (*cross*) FeOOH

Fig. 5 FTIR spectrum of *a* Fe$_3$O$_4$, *b* Fe$_3$O$_4$/SiO$_2$, *c* Fe$_3$O$_4$/SiO$_2$-SO$_3$H

Table 1 Textural properties of the different solids studied

Solid	S_{BET} $(m^2 g^{-1})$	Pore volume $(cm^3 g^{-1})$	Pore size (nm)
SiO$_2$–SO$_3$H	251	0.45	7.2
Fe$_3$O$_4$	17	0.04	3
Fe$_3$O4/SiO$_2$	65	0.11	8
Fe$_3$O4/SiO2–SO$_3$H	32	0.11	14
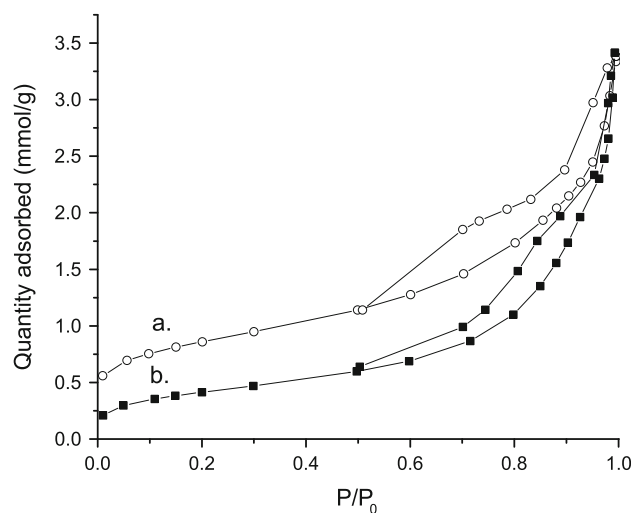
Fig. 6 N$_2$ adsorption–desorption isotherms of *a* Fe$_3$O$_4$/SiO$_2$ and *b* Fe$_3$O$_4$/SiO$_2$-SO$_3$H

Upon functionalization with –SO$_3$H groups, the intensity of the bands at 895 and 795 cm^{-1} also decreases, indicating a possible oxidation of magnetic particles.

Table 1 summarizes the textural properties of the solids obtained from the N$_2$ adsorption–desorption isotherms at 77 K. The functionalization with –SO$_3$H groups slightly decreases the textural properties of commercial SiO$_2$. The Fe$_3$O$_4$ NPs have a relatively low surface area (S_{BET} = 17 m^2/g), but it increases with the silica coating, as shown in Table 1. Figure 6 shows N$_2$ adsorption–desorption isotherms of Fe$_3$O$_4$/SiO$_2$ and Fe$_3$O$_4$/SiO$_2$–SO$_3$H at 77 K. The solids showed type IV isotherms according to the IUPAC classification. In Fig. 6 it can be seen that the process of functionalization with –SO$_3$H groups decreases the pore volume. It has been reported that the textural properties of porous solids decrease drastically when they are treated with organosylanes compounds [44], which indicates that the guest moieties are located inside the pore structure.

The acid capacity of the samples was determined by titration with 0.01 M NaOH (*aq*). The results in terms of mmol H$^+$/g of SO$_3$H groups are listed in Table 2. It is observed that the acidity decreases dramatically with the incorporation of Fe$_3$O$_4$ NPs. A better dispersion of –SO$_3$H

associated with Fe$_3$O$_4$ particles [41]. For all NPs functionalized, the analysis indicated absorption peaks between 540 and 530 cm^{-1} corresponding to the Fe–O vibration related to the magnetite phase [42]. The characteristic absorption bands for Fe–O bond from Fe$_3$O$_4$ are located in the range 375–570 cm^{-1}, but these two bands are shifted to higher values between 440 and 600 cm^{-1}, respectively [43]. Moreover, these bands decrease with the silica coating and subsequent functionalization with sulfonic groups (Fig. 5b, c). The silica coating is evidenced by the appearance of new bands in the spectrum of both Fe$_3$O$_4$/SiO$_2$ (Fig 5b, 1,074 cm^{-1}) and Fe$_3$O$_4$/SiO$_2$-SO$_3$H (Fig. 5c, 1,090 cm^{-1}).

Table 2 Acid capacities by NaOH titration (mmol H/g) and yield (%) to furfural

Catalyst	Acid capacities by NaOH titration of SO_3H (mmol H^+/g)	Yield (%), 4 h
SiO_2–SO_3H	35.8	69
Fe_3O4/SiO_2–SO_3H	7.09	38

Table 3 Furfural yield (%) dehydration in three cycles of reusability

Catalyst	Cycle 1	Cycle 2	Cycle 3
Fe_3O4/SiO_2–SO_3H	38	34	33

groups is observed in solids with a great surface area, indicating a linear relation between surface area and acid capacity.

3.2 Xylose Dehydration to Furfural

The catalytic activity of the solids SO_3H–SiO_2, Fe_3O_4/SiO_2–SO_3H was evaluated in the xylose dehydration reaction (Fig. 1). Table 2 shows the yield for each solid studied. At 4 h all the catalysts showed the formation towards furfural only. The yield was higher in nonmagnetic than in magnetic solids. The yield was higher in nonmagnetic than in magnetic solids, which is attributable to its higher amount of acid sites. The presence of Fe_3O_4 permits an easy separation from the reaction medium, so the reuse of Fe_3O_4/SiO_2–SO_3H was examined after 4 cycles of reaction (Table 3). The results show that the catalytic activity of these catalysts decreased slightly after reuse, maintaining a yield higher than 30 %.

3.3 Furfural Valorization in Multicomponent Reactions

The valorization of furfural using Fe_3O_4/SiO_2–SO_3H as catalyst was studied in two different multicomponent reactions (Biginelli and Hantzsch reactions) in order to prepare different kinds of functionalized nitrogen heterocycles: 3,4-dihydropyrimidin-2(1*H*)-ones (compounds **1, 2**); 3,4-dihydropyrimidin-2(1*H*)-thiones (compounds **3, 4**); trifluoromethylhexahydropyrimidin-2(1*H*)-ones (compounds **5, 6**); trifluoromethylhexahydropyrimidin-2(1*H*)-thiones (compounds **7, 8**); and 1,4-dihydropyrimidines (compounds **9, 10, 11**).

3.3.1 Synthesis of 3,4-Dihydropyrimidin-2(1H)-ones (thiones)

We explored the catalytic activity of Fe_3O_4/SiO_2–SO_3H for the Biginelli reaction, under solvent-free conditions, using

furfural, ethyl or methyl acetoacetate and urea or thiourea (Fig. 7).

Several reaction conditions were checked: temperature, reaction time, amount of catalyst and its reuse in order to obtain the best reaction conditions. The optimized reaction conditions were: a ratio of aldehyde/ethyl or methyl acetoacetate/urea or thiourea (1:1:1.5), 25 mg of catalyst, reaction temperature: 80 °C, and reaction time: 1.5 h. The results are summarized in Table 4.

In all the cases, the reaction proceeded smoothly, and furfural reacted efficiently to give very good to excellent yields of the desired 3,4-dihydropyrimidin-2-(1H)-ones (thiones).

We also investigated the reuse of the catalyst. For this purpose, after completion of the reaction, the obtained mixture was stirred with acetone and then the acetone solution was filtered from the insoluble catalyst (3 × 1 mL). The catalyst was dried under vacuum (293 K) and reused, repeating this procedure. The product yields for the first and second reuses were 90 and 88 %, respectively.

3.3.2 Synthesis of Trifluoromethylhexahydropyrimidin-2(1H)-ones (thiones)

Also, we explored the catalytic activity of Fe_3O_4/SiO_2–SO_3H for the Biginelli reaction, under solvent-free conditions, using furfural, ethyl or methyl acetoacetate and urea or thiourea (Fig. 8). The optimized reaction conditions were: a ratio of furfural/ethyl trifluoromethylacetoacetate/urea or thiourea (1:1:1.5), 25 mg of catalyst, 353 K, and 1.5 h. The results are summarized in Table 5. In the two cases the corresponding trifluoromethylhexahydropyrimidine (Table 5, entries 5 and 6) was the only reaction product formed with 81 and 91 % yield for a reaction time of 1.5 h.

In general, the Biginelli synthesis of 3,4-dihydropyrimidin-2(1H)-ones (thiones) and hexahydropyrimidin-2(1H)-ones (thiones) gives slightly higher yields when urea is used instead the thiourea, in the same reaction condition. (see Table 4, entries 1–4 and Table 5, entries 1–2). This can be justified based on the proposed mechanism by Oliver Kappe which proposes that the first step of the Biginelli reaction, the acid catalyzed formation of acyl imine intermediate formed by the reaction of aldehyde with urea or thiourea, is the rate-determining step [45]. As urea is more nucleophilic than thiourea, is also more reactive and produce yields reaction slightly more high in the same reaction time.

3.3.3 Synthesis of 1,4-Dihydropyrimidines

Finally, we explored the catalytic activity of Fe_3O_4/SiO_2–SO_3H for the Hantzsch reaction, under solvent-free conditions, using furfural, ethyl or methyl acetoacetate
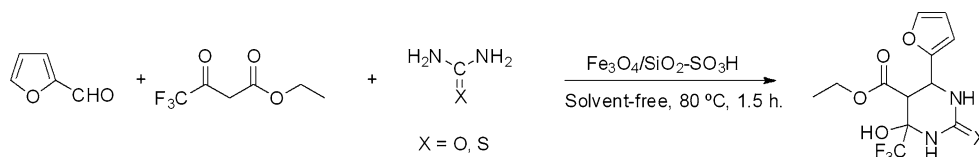
Fig. 7 Synthesis of 3,4-dihydropyrimidin-2(1H)-ones (thiones)
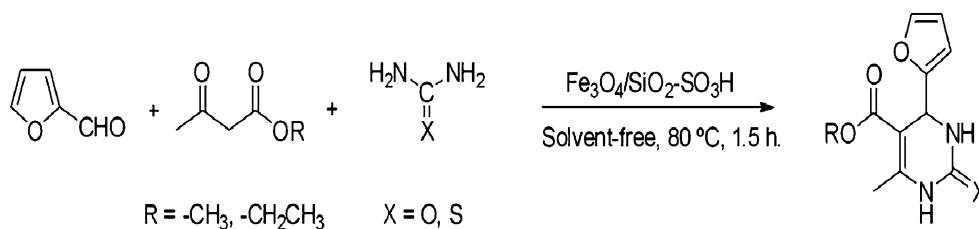
Table 4 Synthesis of 3,4-dihydropyrimidin-2(1H)-ones (thiones)

Entry	Keto ester	Nitrogen source	Product	Yields (%)[a]
1	Methyl acetoacetate	Urea		89 (88,87)[b]
2	Ethyl acetoacetate	Urea		90
3	Methyl acetoacetate	Thiourea		83
4	Ethyl acetoacetate	Thiourea		82

Reaction conditions: a ratio of aldehyde/ethyl or methyl acetoacetate/urea or thiourea (1:1:1.5), 20 mg of catalyst, reaction temperature: 80°C, and reaction time:1.5 h

[a] The conversion was 100 % and the yields correspond at the isolated pure product

[b] First and second reuses

Fig. 8 Synthesis of trifluoromethylhexahydropyrimidinones (thiones)

and ammonium acetate o aniline as nitrogen source (Fig. 9).

After some experiments, we found a set of conditions that generally provide 1,4 dihydropyridines in good yields. The results are listed in Table 6. The experiments were carried out under solvent-free conditions, in the presence of 25 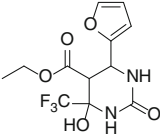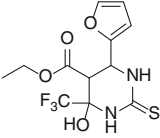mg of catalyst. The temperature and molar ratio of the Fe$_3$O$_4$/SiO$_2$–SO$_3$H acid to substrates were checked to optimize the reaction. The reactions were completed within 1 h at 80 °C, and the crude products were obtained by magnetic separation of the catalyst and evaporation from the acetone solution product. In all the cases, the desired products were obtained with high selectivity, almost free of secondary products.

Recycling of the catalyst was checked in two consecutive batches after the first one; the catalysts showed almost constant activity. The catalyst was separated applying a magnetic field and then washed in polar media such as acetone and no leaching was observed. The use of an insoluble catalyst instead of soluble inorganic acids contributes to waste reduction.

All products listed in Tables 4, 5 and 6 were characterized by ^{1}H NMR and ^{13}C NMR and melting point determination.

4 Conclusions

The magnetic response and acid capacity of Fe_3O_4/SiO_2 drops drastically when the solids are functionalized with MPTMS and subsequently/further oxidized with H_2O_2; however, these solids can be easily separated from the reaction medium applying a magnetic field and act as excellent catalysts in the conversion of xylose to furfural. Moreover, very simple and convenient catalytic methods were developed for the preparation of 3,4-dihydropyrimidinones, 1,4-dihydropyrimidines and fluorinated hexahydropyrimidine derivatives from a multicomponent reaction, under solvent-free conditions using Fe_3O_4/SiO_2–SO_3H catalyst. The procedures have the advantages of low environmental impact, high yields, high selectivity, short reaction time, and easy separation of the catalyst.

Table 5 Synthesis of hexahydropyrimidin-2(1H)-ones (thiones)

Compound	Nitrogen source	Product	Yields (%)
5	Urea		90
6	Thiourea		81

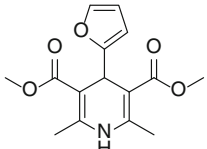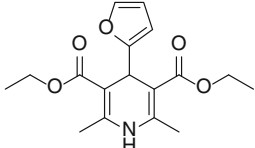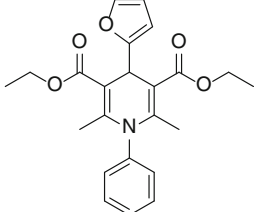Reaction conditions: a ratio of aldehyde/trifuoromethylacetoacetate/urea or thiourea (1:1:1.5), 20 mg of catalyst, reaction temperature: 80 °C, and reaction time: 1.5 h

[a] The conversion was 100 % and the yields correspond at the isolated pure product

Fig. 9 Synthesis of 1,4-dihydropyridines
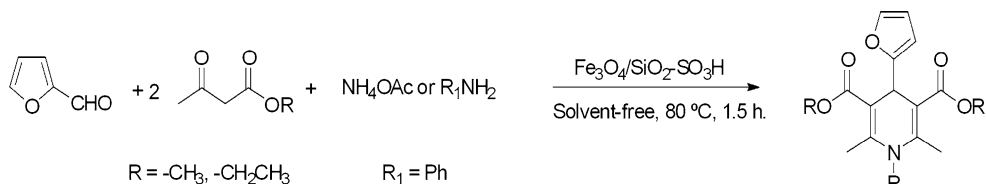
Table 6 Synthesis of 1,4-dihydropyridines

Entry	Keto ester	Nitrogen source	Product	Yields (%)[a]
9	Methyl acetoacetate	Ammonium acetate		91 (88, 88)
10	Ethyl acetoacetate	Ammonium acetate		90
11	Ethyl acetoacetate	Aniline		85

Reaction conditions: a ratio of furfural/methyl or ethyl acetoacetate/ammonium acetate or aniline (1:2:1.2), 20 mg of catalyst, reaction temperature: 80°C, and reaction time: 1.5 h

[a] The conversion was 100 % and the yields correspond at the isolated pure product

References

1. Jeong GH, Kim EG, Kim SB, Park ED, Kim SW (2011) Microporous Mesoporous Mater 144:134
2. Nandan D, Sreenivasulu P, Sivakumar Konathala LN, Kumar M, Viswanadham N (2013) Microporous Mesoporous Mater 179:182
3. Dias AS, Pillinger M, Valente AA (2005) J Catal 229:414
4. Nemati F, Heravi MM, Saeedi Rad R (2012) Chin J Catal 33:1825
5. Anastas PT, Zimmerman JB (2003) Environ Sci Technol 37:94A
6. Wang X, Cheng S, Chan JCC (2007) J Phys Chem C 111:2156
7. Shylesh S, Sharma S, Mirajkar SP, Singh AP (2004) J Mol Catal A 212:219
8. Yamaguchi D, Kitano M, Suganuma S, Nakajima K, Kato H, Hara M (2009) J Phys Chem C 113:3181
9. Rosatella AA, Simeonov SP, Frade RFM, Afonso CAM (2011) Green Chem 13:754
10. Wu L, Yin Z (2013) Carbohydr Res 365:14
11. Maggi R, Piscopo CG, Sartori G, Storaro L, Moretti E (2012) Appl Catal A 411–412:146
12. Shaterian HR, Hosseinian A, Ghashang M (2008) Synth Commun 38:4097
13. Lai D-M, Deng L, Li J, Liao B, Guo Q-X, Fu Y (2011) ChemSusChem 4:55
14. Mrowczynski R, Nan A, Liebscher J (2014) RSC Advan 4:5927
15. Okoli C, Sanchez-Dominguez M, Boutonnet M, Järås S, Civera C, Solans C, Kuttuva GR (2012) Langmuir 28:8479
16. Huber DL (2005) Small 1:482
17. Martínez JJ, Rojas H, Vargas L, Parra C, Brijaldo MH, Passos FB (2014) J Mol Catal A 383–384:31
18. Schätz A, Reiser O, Stark WJ (2010) Chem Eur J 16:8950
19. Singh MS, Chowdhury S (2012) RSC Advan 2:4547
20. Isambert N, Sanchez Duque Mdel M, Plaquevent JC, Genisson Y, Rodriguez J, Constantieux T (2011) Chem Soc Rev 40:1347
21. Kappe CO (2000) Eur J Med Chem 35:1043
22. D'alessandro O, Sathicq A, Palermo V, Sanchez L, Thomas H, Vazquez P, Constantieux T, Romanelli G (2012) Curr Org Chem 16:2763
23. Kappe CO, Falsone F, Fabian WM, Belaj F (1999) Heterocycles 51:77
24. Agbaje OC, Fadeyi OO, Fadeyi SA, Myles LE, Okoro CO (2011) Bioorg Med Chem Lett 21:989
25. Sathicq A, Romanelli P, Ponzinibbio G, Baronetti T, Thomas HJ (2010) Lett Org Chem 7:511
26. Zamani F, Izadi E (2013) Catal Commun 42:104
27. Zamani F, Hosseini SM, Kianpour S (2013) Solid State Sci 26:139
28. Koukabi N, Kolvari E, Zolfigol MA, Khazaei A, Shaghasemi BS, Fasahati B (2012) Advan Synth Catal 354:2001
29. Kang YS, Risbud S, Rabolt JF, Stroeve P (1996) Chem Mater 8:2209
30. Luo B, Song XJ, Zhang F, Xia A, Yang WL, Hu JH, Wang CC (2010) Langmuir 26:1674
31. Testa ML, La Parola V, Liotta LF, Venezia AM (2013) J Mol Catal A 367:69
32. Fu N-Y, Yuan Y-F, Cao Z, Wang S-W, Wang J-T, Peppe C (2002) Tetrahedron 58:4801
33. Vijay K, Ganapaty S, Srinivas Rao A (2010) Asian J Chem 22:2518
34. Zohdi HF, Rateb NM, Elnagdy SM (2011) Eur J Med Chem 46:5636
35. Ghosh PP, Paul S, Das AR (2013) Tetrahedron Lett 54:138
36. Kidwai M, Mohan R (2004) Can J Chem 82:427
37. Wu Y, Zhang T, Zheng Z, Ding X, Peng Y (2010) Mater Res Bull 45:513
38. Musić S, Krehula S, Popović S, Skoko Ž (2003) Mater Lett 57:1096
39. Wang S, Mulligan CN (2008) Environ Inter 34:867
40. Legodi MA, de Waal D (2007) Dyes Pigment 74:161
41. Chen X, Zhu J, Chen Z, Xu C, Wang Y, Yao C (2011) Sens Actuators B 159:220
42. Li W, Zhang B, Li X, Zhang H, Zhang Q (2013) Appl Catal A 459:65
43. Nechifor A, Stoian M, Voicu S, Nechifor G (2010) Optoelect Adv Mat Rap Commun 4:1118
44. Kureshy RI, Ahmad I, Khan N-UH, Abdi SHR, Pathak K, Jasra RV (2006) J Catal 238:134
45. Kappe CO (1997) J Org Chem 62:7201